OXFORD

Human Molecular Genetics, 2020, Vol. 29, No. 3 394–406

doi: 10.1093/hmg/ddz299
Advance Access Publication Date: 21 December 2019
General Article One

GENERAL ARTICLE ONE

Rhodopsin signaling mediates light-induced photoreceptor cell death in *rd10* mice through a transducin-independent mechanism

Jesse C. Sundar[1], Daniella Munezero[2], Caitlyn Bryan-Haring[1], Thamaraiselvi Saravanan[2], Angelica Jacques[2] and Visvanathan Ramamurthy[1,2,3,*]

[1]Departments of Biochemistry, Robert C. Byrd Health Sciences Center, West Virginia University, Morgantown, WV 26505, USA, [2]Departments of Ophthalmology and Visual Sciences, Robert C. Byrd Health Sciences Center, West Virginia University, Morgantown, WV 26505, USA and [3]Departments of Neuroscience, Robert C. Byrd Health Sciences Center, West Virginia University, Morgantown, WV 26505, USA

*To whom correspondence should be addressed at: Department of Ophthalmology and Visual Sciences, West Virginia University School of Medicine, 1 Medical Center Dr, Morgantown, WV 26505, USA. Tel: +1 3045986940; Fax: +1 3045986938; Email: ramamurthyv@mix.wvu.edu

Abstract

Retinitis pigmentosa (RP) is a debilitating blinding disease affecting over 1.5 million people worldwide, but the mechanisms underlying this disease are not well understood. One of the common models used to study RP is the retinal degeneration-10 (*rd10*) mouse, which has a mutation in *Phosphodiesterase-6b* (*Pde6b*) that causes a phenotype mimicking the human disease. In *rd10* mice, photoreceptor cell death occurs with exposure to normal light conditions, but as demonstrated in this study, rearing these mice in dark preserves their retinal function. We found that inactivating rhodopsin signaling protected photoreceptors from degeneration suggesting that the pathway activated by this G-protein-coupled receptor is causing light-induced photoreceptor cell death in *rd10* mice. However, inhibition of transducin signaling did not prevent the loss of photoreceptors in *rd10* mice reared under normal light conditions implying that the degeneration caused by rhodopsin signaling is not mediated through its canonical G-protein transducin. Inexplicably, loss of transducin in *rd10* mice also led to photoreceptor cell death in darkness. Furthermore, we found that the *rd10* mutation in *Pde6b* led to a reduction in the assembled PDE6$\alpha\beta\gamma_2$ complex, which was corroborated by our data showing mislocalization of the γ subunit. Based on our findings and previous studies, we propose a model where light activates a non-canonical pathway mediated by rhodopsin but independent of transducin that sensitizes cyclic nucleotide gated channels to cGMP and causes photoreceptor cell death. These results generate exciting possibilities for treatment of RP patients without affecting their vision or the canonical phototransduction cascade.

Introduction

Retinitis pigmentosa (RP; OMIM: 268000) is a debilitating genetic disorder characterized by night blindness and decreased visual fields, which can progress to complete blindness, and is often accompanied by severe photoreceptor cell loss (1). Mutations in more than 50 genes lead to various forms of this disease, and the two most commonly affected genes that lead to autosomal

Received: August 16, 2019. **Revised:** November 22, 2019. **Accepted:** December 2, 2019

recessive RP are in the *Usher syndrome type-2a* (*Ush2a*) and *Phosphodiesterase-6* (*Pde6*) genes with *Pde6* mutations accounting for 36 000 cases of RP (2). Current therapies available for hereditary RP symptoms are often insufficient and include vitamin A supplementation and wearing sunglasses (3,4). The biochemical mechanisms underlying photoreceptor cell death and subsequent vision loss in RP are not fully understood, and elucidating these mechanisms will aid in the development of more personalized approaches for treating patients with this disease.

One of the commonly used animal models of RP is the retinal degeneration-10 (*rd10*) mouse where visual function is gradually lost and is accompanied by photoreceptor cell death (5). This phenotype closely mimics the human form of the disease. This mouse model has a missense mutation in the catalytic β subunit of the PDE6 holoenzyme (mutation denoted as PDE6$\beta^{rd10/rd10}$, i.e. *rd10* hereafter) (5). *Rd10* animals raised under normal light conditions in a vivarium with a 12 h light/12 h dark cycle show complete degeneration of the photoreceptor outer nuclear layer (ONL) by postnatal day 45 (PN45). Intriguingly, our studies show that *rd10* mice reared in complete darkness show significant preservation of the ONL at PN45. Elucidating the mechanism behind this light-dependent photoreceptor cell death in the *rd10* mouse may lead to new insights into the human form of the disease in addition to development of better treatments for autosomal recessive RP.

We hypothesized that the biochemical signaling cascade underlying sensation to light plays a key role in the light-dependent degeneration of photoreceptors in the *rd10* mouse model. The phototransduction cascade is fundamental to vision in all mammalian species and begins when the light-sensing G-protein-coupled receptor (GPCR) rhodopsin is activated by the absorption of a photon through its chromophore 11-*cis* retinal. The subsequent conformational change in rhodopsin leads to activation of the heterotrimeric G-protein transducin. The α subunit of transducin then activates the effector enzyme of the phototransduction cascade PDE6, which leads to closing of cyclic nucleotide gated channels and hyperpolarization of the photoreceptor cell.

After photon absorption, the chromophore 11-*cis* retinal attached to opsin is isomerized to all-*trans* retinal in photoreceptors (6). In a series of enzymatic reactions known as the visual cycle, 11-*cis* retinal is regenerated in the retinal pigment epithelium (RPE) and returned to photoreceptors to restore rhodopsin's photosensitivity (6,7). The visual cycle begins with the reduction of all-*trans* retinal to all-*trans* retinol by NADPH-dependent retinol dehydrogenase (6,8). All-*trans* retinol is then esterified in the RPE by lecithin retinol acyltransferase before being isomerohydrolyzed by the RPE-specific protein of 65 kDa (RPE65), which catalyzes the production of 11-*cis* retinol (6,9). The alcohol 11-*cis* retinol is then oxidized back to the aldehyde 11-*cis* retinal by 11-*cis* retinol dehydrogenase to complete the cycle (6,8). Importantly, the RPE65 enzyme, among other critical visual cycle components, becomes necessary for the regeneration of rhodopsin's photosensitivity, and without this enzyme, photoreceptors are essentially rhodopsin-deficient (10).

The absence of RPE65 (*Rpe65*−/−) prevents apoptosis of photoreceptors in mice exposed to high-intensity light (15 000 lux) (11). These findings suggest a role for activated rhodopsin in photoreceptor degeneration in response to light exposure. We predicted that a similar signaling cascade is involved in photoreceptor cell death in *rd10* mice. We also wanted to know if this rhodopsin signaling requires transducin for apoptotic signaling in *rd10* mouse photoreceptors.

To test this hypothesis, mice lacking functional rod transducin-α alleles (*Gnat1*−/−) and mice lacking functional *Rpe65* alleles (*Rpe65*−/−) were crossed with *rd10* mice to generate *Gnat1*−/− *rd10* and *Rpe65*−/− *rd10* experimental mice (10,12). Ablation of RPE65 inactivates rhodopsin signaling since it is required for regeneration of rhodopsin's chromophore 11-*cis* retinal (10). A rhodopsin knockout mouse could not be used because photoreceptor degeneration is observed, and outer segments (OSs) fail to develop properly in this mouse model (13).

After validating the *Gnat1*−/− *rd10* and *Rpe65*−/− *rd10* mice, we found that the lack of functional transducin failed to prevent light-induced photoreceptor cell death in *rd10* mice and, to our surprise, led to degeneration in dark. Indeed, we found that removal of *Rpe65* delays photoreceptor cell death in *rd10* mice reared under normal light conditions. In addition, we found that the levels of the functional PDE6$\alpha\beta\gamma_2$ heterotetramer were highly reduced. Lastly, we observed that the levels of each individual subunit of PDE6 were decreased in *rd10* mice in addition to mislocalization of PDE6γ.

Results

Dark rearing *rd10* mice delays photoreceptor cell death

Mice homozygous for the *rd10* mutation were raised from birth in either complete darkness or in a vivarium with a 12 h ∼175 lux light: 12 h dark cycle. At PN45, whole eyes from these mice were collected along with *C57BL6/J* controls for histological analysis of the retinal ONL by hematoxylin and eosin (H&E) staining and immunofluorescence microscopy. *Rd10* mice raised in normal cyclic light conditions experienced substantial photoreceptor degeneration (Fig. 1A and B). In contrast, there was significant preservation of the ONL in *rd10* mice raised in complete darkness with approximately three to four layers of photoreceptor nuclei remaining at PN45 (Fig. 1A and B). These findings suggest that the *rd10* mutation sensitizes photoreceptors to light and makes them susceptible to cell death. As shown in Fig. 1A, no substantial changes were observed in the RPE or inner retinal layers (inner nuclear layer and ganglion cell layer) between *rd10* mice raised in complete darkness and under normal light conditions. Overall, our findings show significant preservation of photoreceptors in dark reared *rd10* animals.

Retinal function is preserved in dark reared *rd10* mice

We next sought to determine if the surviving photoreceptors are functional in dark reared *rd10* mice in early adulthood at PN45. One of the commonly used methods for determination of photoreceptor function is electroretinography (ERG) where electrical activity originating from the neural retina is measured after exposure to a light stimulus. This technique allows for analysis of both rod and cone photoreceptor function. Indeed, the preservation of the ONL in *rd10* mice raised in complete darkness correlated with increased photoreceptor function in contrast to *rd10* mice raised under cyclic light conditions (Fig. 2A–D). ERG traces of the cyclic light reared *rd10* mice revealed a complete absence of 'a' and 'b' waves in contrast to dark reared *rd10* mice and age-matched C57BL6/J controls under both scotopic and photopic conditions (Fig. 2A and B). Scotopic ERGs at varying light intensities confirmed the increased 'b'-wave amplitude in dark reared *rd10* mice in contrast to *rd10* mice raised under cyclic light conditions, which suggest that functional rod photoreceptor neurons are preserved in these mice (Fig. 2C). Similarly, photopic ERGs of the cyclic light and dark reared *rd10*

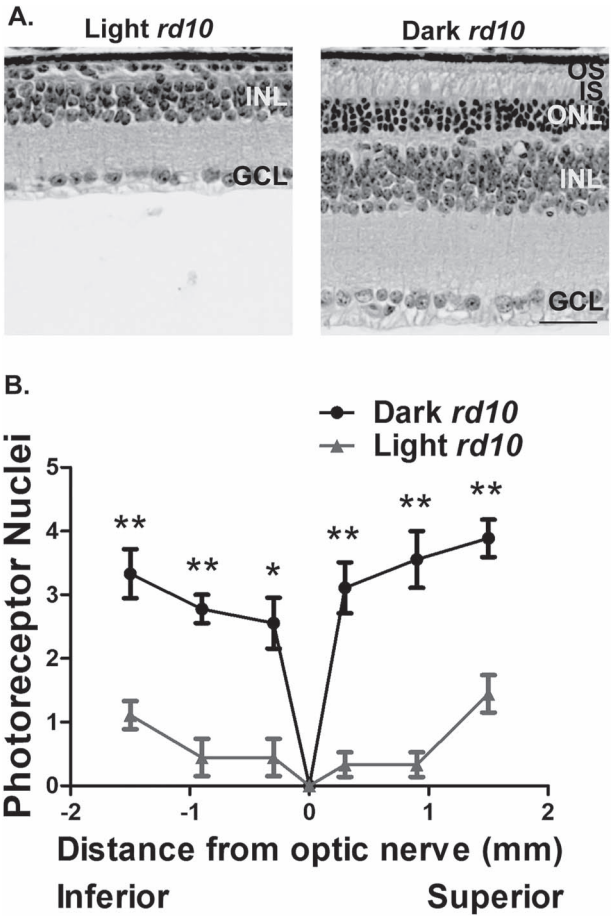

Figure 1. Dark rearing delays photoreceptor cell death in *rd10* animals. **(A)** Brightfield images of H&E stained retinal cross sections from the PN45 *rd10* mice reared under standard light conditions and in darkness (OS, outer segment; IS, inner segment; ONL, outer nuclear layer; INL, inner nuclear layer; GCL, ganglion cell layer). Scale bar = 30 μm. **(B)** Spider diagram showing the quantification of the ONL thickness at six regions from the inferior to superior retina in the light and dark reared *rd10* mice at PN45 ($n = 3$). Data are shown as the mean ± standard error of the mean (SEM) with statistical significance calculated using the two-tailed homoscedastic unpaired student's *t*-test (*$P < 0.05$; **$P < 0.01$).

mice revealed a significantly increased 'b'-wave amplitude in the dark reared *rd10* mice implying that dark rearing preserves cone photoreceptors in these mice (Fig. 2D). When compared to age-matched C57BL6/J wild-type controls, we saw a reduction in both 'a'-wave and 'b'-wave amplitudes in the dark reared *rd10* mice under scotopic but not photopic testing conditions (Fig. 2A–D). This is likely due to the mutation in the rod-specific PDE6β subunit, which affects the levels of the rod-specific PDE6 holoenzyme (Fig. 5).

Inactivating transducin does not prevent light-induced photoreceptor cell death in *rd10* mice

To determine if transducin was involved in the mediation of this light-dependent photoreceptor cell death in the *rd10* mouse, we crossed *rd10* mice with the *Gnat1*−/− mouse model. The *Gnat1*−/− mouse lacks a functional rod transducin-α gene (*Gnat1*) and yet experiences almost no photoreceptor degeneration due to the loss of transducin (12). *Gnat1*+/− *rd10* × *Gnat1*+/− *rd10* crosses were used to generate *Gnat1*−/− *rd10* knockout mice and *rd10* littermate control mice. The loss of rod transducin-α subunit (GαT1) was validated by western blot. GαT1 was absent in retinal extracts of *Gnat1*−/− *rd10* double knockout mice (Fig. 3A). The litters from the heterozygous crosses were raised in either cyclic light or complete darkness for 45 days. H&E stained retinal sections and immunofluorescence microscopy were used to analyze the retinal morphology. At PN45, photoreceptor cell death is seen in both the normal light reared *Gnat1*+/+ *rd10* and *Gnat1*−/− *rd10* animals suggesting that transducin is not mediating the light-dependent photoreceptor cell death (Fig. 3B and D). To our surprise, dark rearing *Gnat1*−/− *rd10* mice failed to preserve photoreceptors and caused substantial photoreceptor degeneration with almost no ONL nuclei left at PN45 (Fig. 3C and E). Overall, these findings suggest that the light-dependent photoreceptor cell death observed in *rd10* mice occurs through a transducin-independent mechanism.

Inactivating *Rpe65* protects *rd10* mice from light-induced photoreceptor cell death

To determine if the activation of rhodopsin is mediating the light-dependent photoreceptor cell death in *rd10* animals, we inactivated rhodopsin by blocking the recycling of its chromophore 11-*cis* retinal with the use of the *Rpe65*−/− mouse model (10). A 11-*cis* retinal is regenerated from all-*trans* retinal in part by RPE65, a retinol isomerase encoded by the *Rpe65* gene (10). We crossed *Rpe65*−/− mice with *rd10* mice to ultimately develop *Rpe65*−/− *rd10* knockout mice and littermate control *rd10* mice. We then validated these mice by immunofluorescence microscopy (Fig. 4A). As expected, RPE65 (green) was absent in the *Rpe65*−/− *rd10* knockouts. Litters from heterozygous crosses were then raised in either normal light or complete darkness for 45 days before mice were sacrificed and whole eyes were collected for histological analysis. H&E and immunostaining of retinal sections were then imaged to analyze the retinal morphology. At PN45, significant photoreceptor cell death is seen in the normal light reared *Rpe65*+/+ *rd10* mice (Fig. 4B and D). Strikingly, however, standard light reared *Rpe65*−/− *rd10* mice experience a slower rate of photoreceptor cell death with approximately three layers remaining at PN45 (Fig. 4B and D). When these mice were raised in complete darkness, photoreceptor nuclei were preserved to a similar extent between *rd10* mice and *Rpe65*−/− *rd10* mice as seen by similar ONL thickness (Fig. 4C and E). Altogether, these findings suggest that rhodopsin is signaling independently of transducin to mediate the light-dependent photoreceptor cell death in the *rd10* mouse.

The functional PDE6 holoenzyme is reduced and misassembled

We next wanted to test how the *rd10* mutation in the β subunit of PDE6 affects the assembly of the holoenzyme. To this end, we immunoprecipitated the PDE6 complex with ROS1 antibody, which specifically detects the assembled functional PDE6 holoenzyme (14), in *rd10* and *C57BL6/J* control retinal lysates at PN15 before the onset of photoreceptor degeneration (Fig. 5A). We then immunoblotted the fractions from the immunoprecipitation and probed with antibodies directed against PDE6α, PDE6β and PDE6γ to check for the assembly of each subunit to the complex. Interestingly, in *rd10* mice, the levels of all three PDE6 subunits are considerably reduced in the bound (assembled)

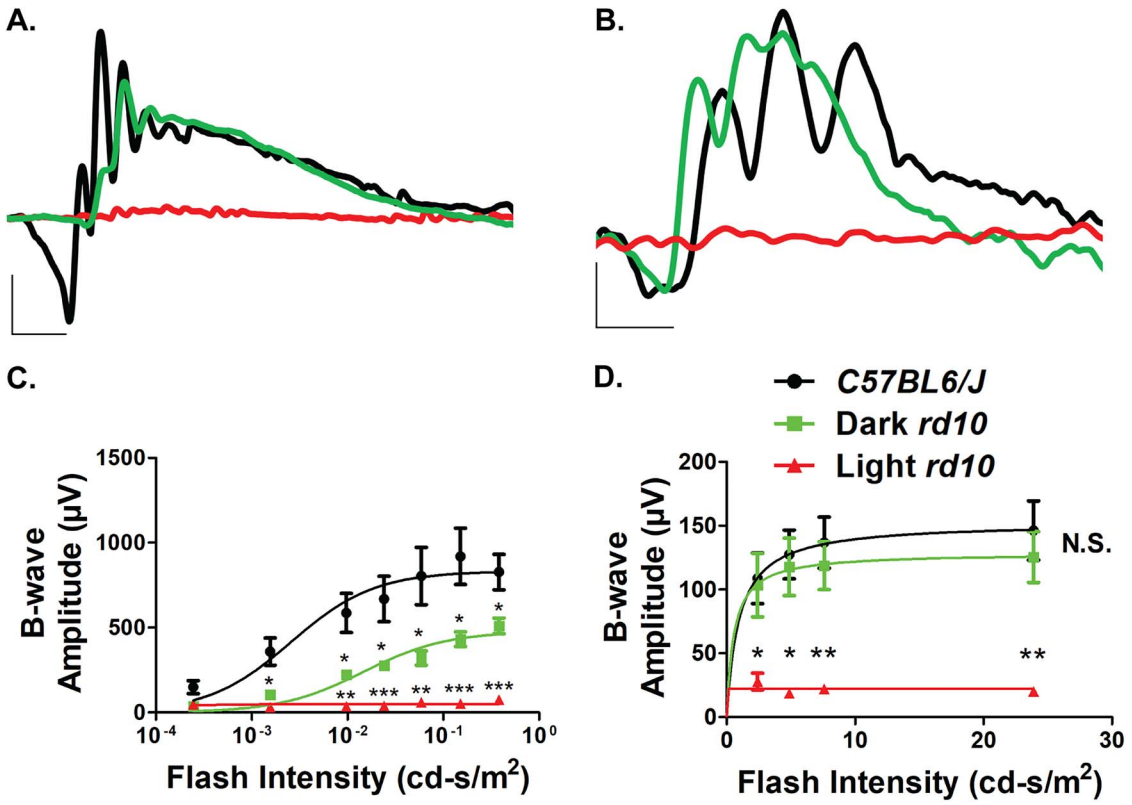

Figure 2. Preservation of retinal function in dark reared *rd10* mice. **(A)** Representative scotopic (0.151 cd-s/m^2) ERGs of the standard light (red) and dark (green) reared *rd10* mice at PN45 along with age-matched C57BL6/J controls (black) after overnight dark adaptation (Scotopic scale bar: *x*-axis = 20 ms, *y*-axis = 200 μV). **(B)** Representative photopic (7.6 cd-s/m^2) ERGs of the standard light (red) and dark (green) reared *rd10* mice along with age-matched C57BL6/J controls (black) under light-adapted conditions using a 30 cd-s/m^2 rod-saturating white background light at PN45 (Photopic scale bar: *x*-axis = 20 ms, *y*-axis = 40 μV). **(C)** Light stimulus intensity plot of the scotopic 'b'-wave response from the standard light and dark reared *rd10* mice along with age-matched C57BL6/J controls at PN45 ($n = 3$). The dose response relationship was modeled using the Naka-Rushton fit with maximum amplitudes determined to be 833 ± 64, 479 ± 31 and 50 ± 5 μV for the wild-type, dark and light reared *rd10* mice, respectively. **(D)** Light stimulus intensity plot of the photopic 'b'-wave response from the dark and standard light reared *rd10* mice along with age-matched C57BL6/J controls at PN45 ($n = 3$). The dose response relationship was modeled using the Naka-Rushton fit with maximum amplitudes determined to be 153 ± 20, 129 ± 19 and 22 ± 4 μV for the wild-type, dark and light reared *rd10* mice, respectively. Data are shown as the mean ± SEM with statistical significance calculated using the two-tailed homoscedastic unpaired student's *t*-test (*$P < 0.05$; **$P < 0.01$; ***$P < 0.001$).

fraction in contrast to age-matched *C57BL6/J* controls suggesting that there is a decrease in the amount of assembled, functional PDE6 (Fig. 5A). Furthermore, significant amounts of the PDE6γ subunit are present in the unbound (unassembled) fraction in *rd10* mice with no enrichment of PDE6γ in the bound (assembled) fraction as seen in the age-matched *C57BL6/J* controls (Fig. 5A). These data suggest that the PDE6 holoenzyme is misassembled, and there is a likely dysregulation of PDE6 if the γ subunit is unable to interact with the α and β subunits.

The *rd10* mutation alters levels of the PDE6 subunits

We next wanted to determine if the reduction in the assembled PDE6 holoenzyme in *rd10* mice was due to an instability of the complex or a reduction in the steady-state protein levels of the individual subunits. Immunoblotting of retinal lysates from *rd10* mice revealed that the levels of the PDE6β subunit are dramatically reduced prior to photoreceptor degeneration (Fig. 5B). The drastic loss in PDE6β levels is accompanied by a significant decrease in its cognate partner catalytic PDE6α subunit (Fig. 5B) implying that the ability for cGMP hydrolysis and consequently phototransduction efficiency is greatly reduced. Lastly, the levels of the inhibitory γ subunit are also decreased (Fig. 5B). The reduction in PDE6β levels was confirmed by immunofluorescence microscopy of retinal sections from the *rd10* mice before the onset of photoreceptor degeneration (Fig. 5C). Overall, the *rd10* mutation substantially affects the levels of each individual PDE6 subunit.

PDE6γ but not PDE6α is mislocalized in both standard light and dark reared *rd10* mice

After finding PDE6γ in the unassembled fraction of our pull-down experiment, we predicted that the PDE6 subunits may not be properly localized in *rd10* mice. To test this hypothesis, we used immunofluorescence microscopy to examine retinal sections from normal light and dark reared *rd10* mice for PDE6α, PDE6β and PDE6γ localization before the onset of photoreceptor degeneration. Retinal sections were first stained with anti-PDE6β antibody and wheat germ agglutinin (WGA, a rod OS marker) and counterstained with 4′,6-diamidino-2-phenylindole (DAPI) to see how the *Pde6b* mutation affects PDE6β localization. The reduction in PDE6β observed in Fig. 5B was confirmed by immunofluorescence microscopy (Fig. 5C), but its localization remained obscure (Fig. 5C). We found PDE6α to be properly localized to the OS in both normal light and dark reared *rd10* mice (Fig. 6A), and its levels were severely reduced in agreement with Fig. 5B. On the contrary, we observed substantial mislocalization

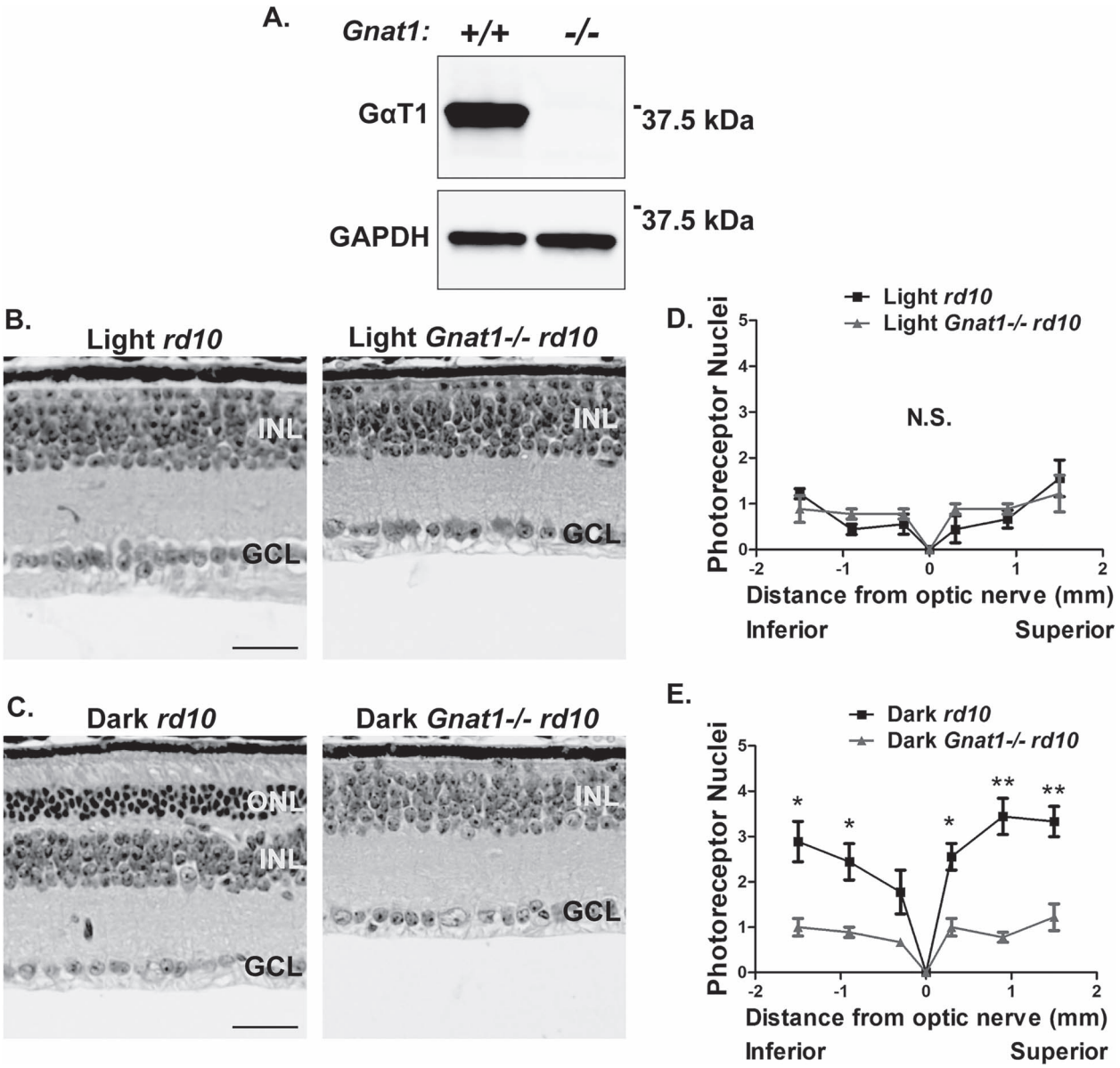

Figure 3. Light-dependent photoreceptor cell death in *rd10* mice is not mediated by transducin signaling. **(A)** Validation of the *Gnat1−/− rd10* mice by immunoblotting retinal lysates and subsequently probing with an antibody against rod transducin-α (GαT1). GAPDH serves as a loading control. Molecular weight in kilodaltons is indicated on the right. **(B)** H&E stained retinal cross sections from the standard light reared *Gnat1−/− rd10* mice along with littermate *rd10* controls at PN45. (OS, outer segment; IS, inner segment; ONL, outer nuclear layer; INL, inner nuclear layer; GCL, ganglion cell layer). Scale bar = 30 µm. **(C)** H&E stained retinal cross sections from the dark reared *Gnat1−/− rd10* mice along with littermate *rd10* controls at PN45. Scale bar = 30 µm. **(D)** Spider plot showing the quantification of the photoreceptor nuclei at six regions from the inferior to superior retina in the standard light reared *Gnat1−/− rd10* mice and littermate *rd10* controls at PN45. **(E)** Quantification of photoreceptor nuclei at six regions from the inferior to superior retina in the dark reared *Gnat1−/− rd10* mice and littermate *rd10* controls at PN45. Data are shown as the mean ± SEM ($n = 3$, two-tailed homoscedastic unpaired student's *t*-test; $^{*}P < 0.05$; $^{**}P < 0.01$; N.S., not significant).

of PDE6γ in both normal light and dark reared *rd10* mice in contrast to the *C57BL6/J* control prior to the onset of photoreceptor degeneration (Fig. 6B). These data suggest that the *rd10* mutation could alter the regulation of the PDE6 holoenzyme through mislocalization of the inhibitory PDE6γ subunit.

Discussion

Our studies reveal that dark rearing prolongs survival and function of rod and cone photoreceptors in the *rd10* mouse model (Figs 1 and 2). We also examined the signaling pathways underlying the light-dependent photoreceptor cell death and the protection afforded by dark-rearing *rd10* mice. Our findings show that the light-induced photoreceptor degeneration caused by the *rd10* mutation is mediated by rhodopsin signaling (Fig. 4). However, the degeneration is independent of the canonical rhodopsin-transducin signaling cascade (Fig. 3). Intriguingly, the protection afforded by dark rearing was lost when transducin signaling was abolished (Fig. 3). However, inhibition of rhodopsin signaling had no substantial effect on photoreceptor survival in dark-reared *rd10* mice (Fig. 4). The *rd10* mutation also caused a significant reduction in the levels of the functional PDE6$\alpha\beta\gamma_2$ heterotetramer in addition to a possible misassembly of PDE6 and a reduction in each of the individual subunits (Fig. 5). Corroborating the misassembly of PDE6, PDE6γ but not PDE6α was mislocalized in both light and dark reared *rd10* mice (Fig. 6). It has been

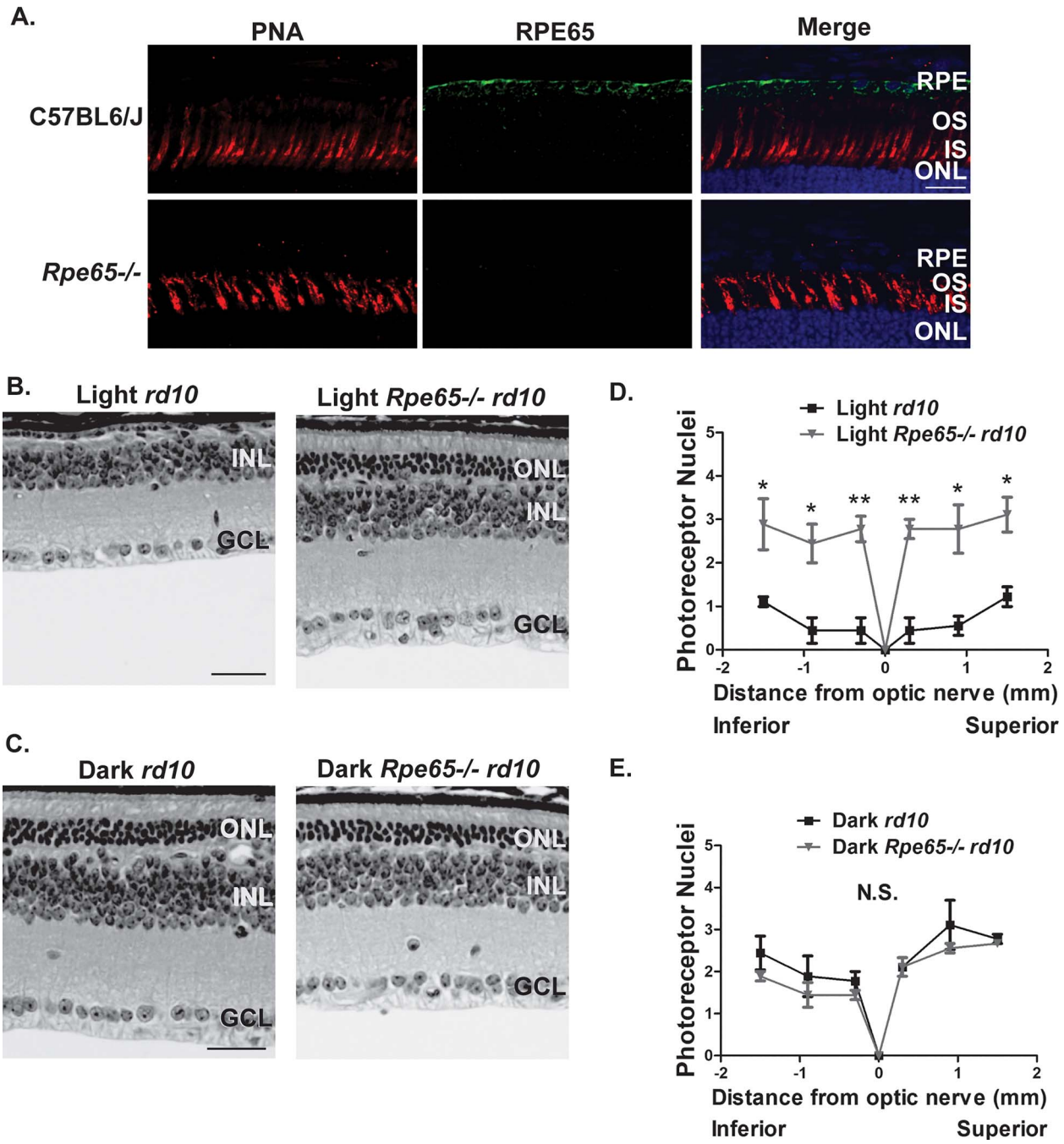

Figure 4. Inactivating Rpe65 protects *rd10* mice from light-induced photoreceptor cell death. **(A)** Validation of the *Rpe65−/− rd10* mice at PN15 before the onset of photoreceptor degeneration by immunofluorescence microscopy of retinal cross sections stained with RPE65 antibody (green), PNA (cone photoreceptor OS marker, red) and DAPI nuclear counterstain (blue). Scale bar = 20 µm. **(B and C)** H&E stained retinal cross sections from the standard light reared (B) and dark-reared (C) *Rpe65−/− rd10* mice along with littermate *rd10* controls at PN45 (OS, outer segment; IS, inner segment; ONL, outer nuclear layer; INL, inner nuclear layer; GCL, ganglion cell layer). Scale bar = 30 µm. **(D)** ONL spider plot showing the quantification of the ONL thickness at six regions from the inferior to superior retina in the light reared *Rpe65−/− rd10* mice and littermate *rd10* controls at PN45. **(E)** ONL spider plot from the inferior to superior retina in the dark reared *Rpe65−/− rd10* mice and littermate *rd10* controls at PN45. Data are shown as the mean ± SEM ($n = 3$, two-tailed homoscedastic unpaired student's *t*-test; $^{*}P < 0.05$; $^{**}P < 0.01$; N.S., not significant).

shown that photoreceptor degeneration caused by mutations in PDE6 such as *rd1* and *rd10* can be genetically rescued by inactivating cyclic nucleotide-gated channels (15,16), but this approach has limited clinical applicability since the phototransduction cascade becomes arrested. Our study reveals that a rhodopsin-mediated signaling event that is independent of transducin is causing cell death in *rd10* mice. Novel therapies can be designed to target this pathway that modulates photoreceptor viability and thus treat patients with RP while not affecting their vision.

The *rd10* mouse model is a widely used mouse model of RP, which carries a missense mutation in exon 13 of the *Pde6b* gene that leads to a substitution of arginine for cysteine (Arg560Cys) in the β subunit of the PDE6 holoenzyme (5). We found that this mutation causes a significant reduction in levels of the

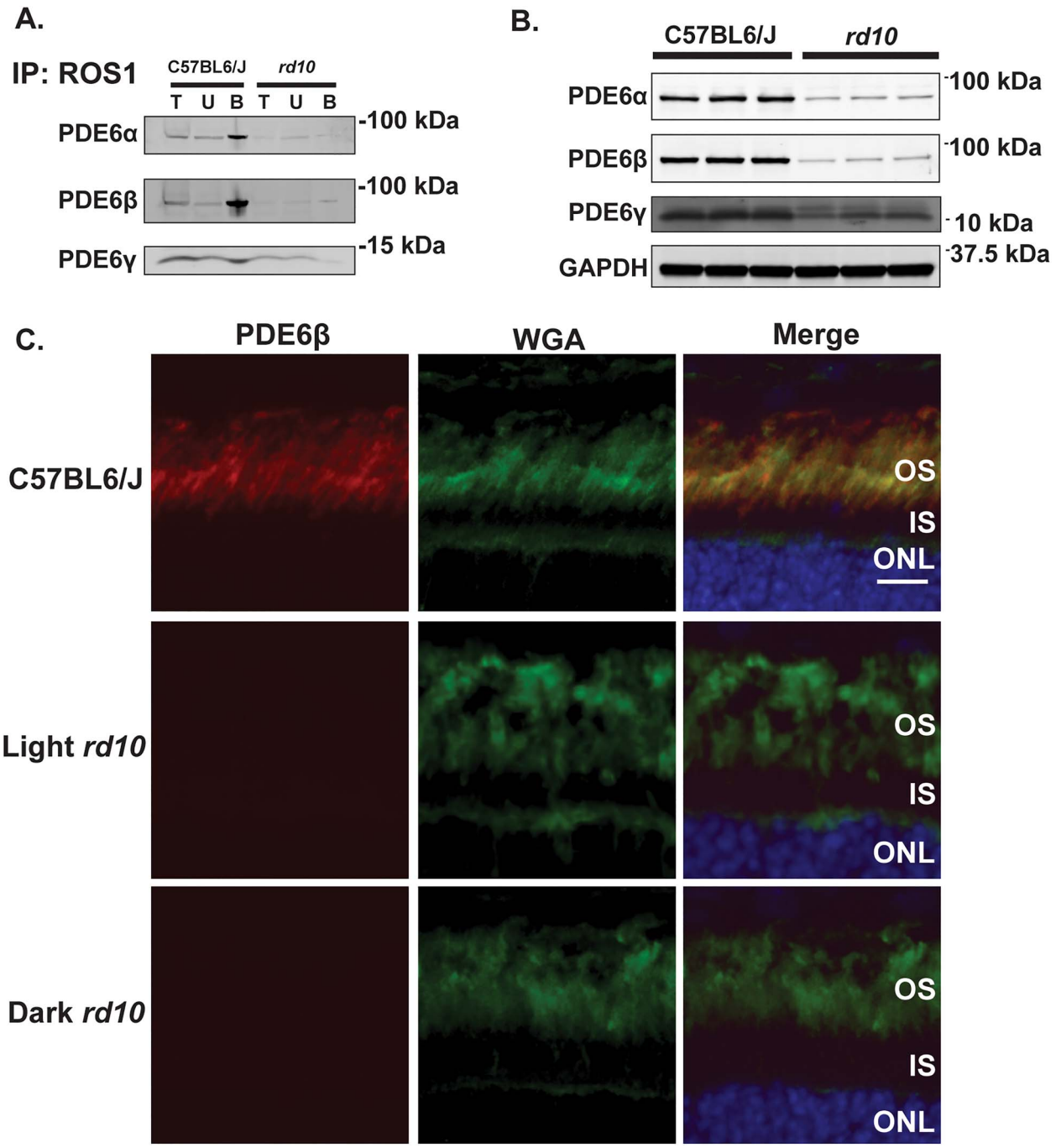

Figure 5. The *rd10* mutation causes a reduction in the levels of the functional PDE6 complex and its individual subunits. **(A)** PN15 C57BL6/J (left) and *rd10* (right) retinal lysates were used for immunoprecipitation by incubation with ROS1 antibody, which recognizes the assembled PDE6$\alpha\beta\gamma_2$ complex. Following immunoprecipitation, total (T), unbound (U) and bound (B) fractions were subjected to size separation by gel electrophoresis and then electroblotted onto PVDF membranes before probing with antibodies directed against either PDE6α, PDE6β, or PDE6γ to check for the assembly of each subunit to the complex. **(B)** Immunoblot of retinal lysates from PN15 C57BL6/J wild-type control mice ($n=3$) and *rd10* mice ($n=3$) probed with antibodies directed against PDE6α, PDE6β, PDE6γ and GAPDH (loading control). **(C)** Immunofluorescence microscopy images of retinal cross sections from C57BL6/J wild-type control mice and light and dark reared *rd10* mice after probing with an antibody directed against PDE6β (red), WGA (rod photoreceptor OS marker shown in green) and DAPI (blue) counterstain. Scale bar = 10 μm.

functional PDE6$\alpha\beta\gamma_2$ holoenzyme in addition to a probable misassembly of PDE6. We found the majority of PDE6γ in the unassembled fraction of *rd10* mice, and PDE6γ was mislocalized in the inner segments (ISs) of *rd10* mice. Similarly, we witnessed a reduction in all three subunits of PDE6 with PDE6α and PDE6β being most dramatically affected. These findings are similar to a recently published study showing that the *rd10* mutation causes an instability of the PDE6 holoenzyme and a subsequent reduction in basal and maximal PDE6 activity (15). Interestingly, inactivation of cyclic nucleotide-gated channels protects *rd10* mice from photoreceptor degeneration implicating Ca^{2+} ion influx as one factor driving cell death (15). Altogether, these findings point to altered regulation of the PDE6 holoenzyme as a cause of degeneration in *rd10* mice.

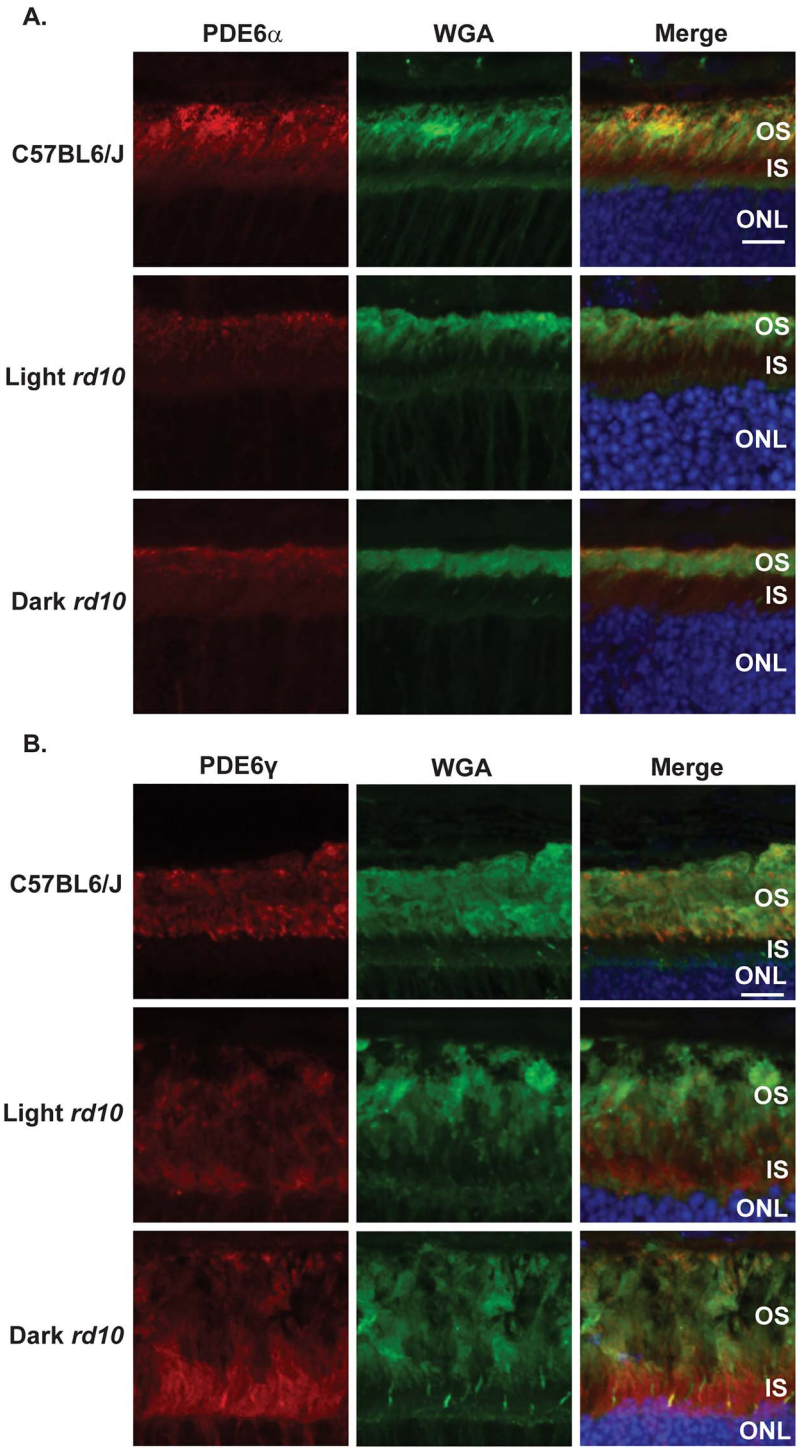

Figure 6. PDE6γ but not PDE6α is mislocalized in both light and dark reared *rd10* mice. **(A)** Immunofluorescence microscopy images of retinal cross sections from the light and dark reared *rd10* mice along with a C57BL6/J wild-type control after probing with antibody directed against PDE6α (red), WGA (rod photoreceptor OS marker shown in green) and DAPI (blue) nuclear counterstain. Scale bar = 10 µm. **(B)** Immunofluorescence microscopy images of retinal cross sections from the light and dark reared *rd10* mice along with a C57BL6/J wild-type control after probing with antibody against PDE6γ (red), WGA (green) and DAPI (blue). Scale bar = 10 µm.

Interestingly, mice lacking the inhibitory PDE6γ subunit have dysregulation of the PDE6 holoenzyme and undergo rapid photoreceptor cell death even in the presence of PDE6$\alpha\beta$ (17). This absence of PDE6γ leads to a paradoxical decrease in PDE6$\alpha\beta$ activity, which causes high cGMP concentrations that likely keep the cGMP-gated cation channels open continuously leading to an excessive cation influx and photoreceptor degeneration (17,18). Alternatively, it is possible that the *rd10* mutation and subsequent PDE6γ mislocalization could lead to protein misfolding and aggregation that can overload the proteasome (19). This idea is supported by findings that show an overload of the proteasome is a common underlying mechanism in many forms of hereditary retinal disease, especially when the causative mutations are in phototransduction genes (19).

After inactivating rhodopsin signaling, we found that photoreceptors were protected in normal light conditions suggesting that rhodopsin is mediating light-accelerated photoreceptor cell death in *rd10* mice. Strikingly, our data also revealed that photoreceptor degeneration in *rd10* mice raised under normal light conditions is independent of transducin-α, which is rhodopsin's canonical interactor. Altogether, these findings lead us to conclude that rhodopsin can signal through other Gi/o-family members besides transducin (T). This conclusion is supported by several other studies, which have suggested that rhodopsin can couple to other members of the Gi/o family (20–24). For instance, one report showed that activated rhodopsin expressed in cell culture inhibited adenylyl cyclase activity through a Gi signaling cascade (20). Another study using primary retinal cell culture found that activation of rhodopsin in the plasma membrane altered the adenylate cyclase cascade to cause photoreceptor cell death (24). Yet, another study found that Gi$\beta\gamma$ can replace T$\beta\gamma$ to restore the rhodopsin-stimulated GTPase activity of Tα, and they also found that Giα exhibited rhodopsin-stimulated GTPase activity when reconstituted with Gi$\beta\gamma$ or T$\beta\gamma$ (23). If rhodopsin's non-canonical G-protein interactor can be identified *in vivo*, it may be possible to treat RP patients without affecting their vision or the canonical phototransduction cascade by targeting this non-canonical subunit. Remarkably, inhibitory drugs targeting G-protein subunits have already been developed and are showing strong efficacy in preclinical models (25).

Likewise, transducin-independent signaling in photoreceptors is well documented (26–29). For example, deletion of *Grk1* led to photoreceptor degeneration, even in the absence of transducin (26). A previous report also showed that photoreceptor cell death caused by bright light is independent of transducin (27). Likewise, transducin signaling was found to not play a direct role in the light-dependent dephosphorylation of GRK1 (29). Another study found that activation of rhodopsin leads to phosphorylation of the insulin receptor, and this is independent of transducin implying that other pathways can be activated through rhodopsin signaling (30). Interestingly, the insulin receptor has been shown to play a neuroprotective role when mice are exposed to light (31). The activated insulin receptor is thought to desensitize cyclic nucleotide-gated channels to the effects of cGMP (32). This would likely result in increased closure of these ion channels and decreased Ca^{2+} entry into the cell.

When we compared our mechanistic findings to other studies of *rd10* mice, we found that the signaling pathways underlying the photoreceptor degeneration observed in *rd10* mice may be complex and multifactorial. For instance, one report found that inhibition of MCP-1 signaling increased photoreceptor viability in *rd10* mice (33). Another study found that inhibition of ceramide-mediated apoptotic signaling reduced photoreceptor cell death in *rd10* mice (34). Interestingly, activation of adenosine monophosphate-activated protein kinase (AMPK) signaling protected photoreceptors in *rd10* mice (35). Likewise, activation of Wnt signaling rescued photoreceptors in *rd10* mice from undergoing severe photoreceptor degeneration (36). A previous report also found that inhibition of $p75^{NTR}$ signaling reduced photoreceptor cell death in *rd10* mice (37). Remarkably, inhibition of TNFα signaling also reduced photoreceptor cell death in *rd10* mice (38). Inhibition of AMPA/kainate signaling was found to increase photoreceptor survival in *rd10* mice as well (39). Perhaps tying multiple pathways together, one group observed that calcium overload and calpain activation occurred in *rd10* mice before the onset of photoreceptor degeneration in addition to an increased permeability of lysosomal membranes (40). Lastly, Nakao *et al*. found that adenylyl cyclase caused photoreceptor cell death in *rd10* mice (41). Altogether, these findings suggest that the mechanisms underlying neurodegeneration in *rd10* mice are complex and multifactorial.

Similarly, multiple studies have shown that various treatment regimens can mitigate the photoreceptor degeneration seen in the *rd10* mouse model. For example, it has been shown that injection of pro-insulin or IGF1 has a neuroprotective effect in *rd10* mice (42,43). Inhibition of microglial phagocytosis by treatment with cRGD also increased photoreceptor survival in *rd10* mice (44). In a similar manner, Granulocyte Colony-Stimulating Factor (G-CSF) and Erythropoietin delayed neurodegeneration in *rd10* mice (45). Interestingly, treatment with either tamoxifen, tauroursodeoxycholic acid, carnosic acid, or Norgestrel reduced photoreceptor cell death in *rd10* mice (46–49). Implicating oxidative stress as one factor driving photoreceptor cell death, treatment with antioxidants such as α-tocopherol and ascorbic acid preserved photoreceptor function in *rd10* mice (50). Suggestive of a dysregulation of iron, injection of transferrin protected *rd10* mice from undergoing severe photoreceptor degeneration (51). This was complemented by another study, which found that treating *rd10* mice with zinc desferrioxamine had a neuroprotective effect (52). Lastly, valosin-containing protein inhibitors and continuous environmental enrichment provided some degree of neuroprotection in *rd10* mice (53–55).

Surprisingly, our findings also reveal that transducin is critical for photoreceptor survival in *rd10* mice reared in complete darkness. It is important to note that the photoreceptor degeneration in the *Gnat1−/− rd10* mice was not caused by the removal of the *Gnat1* since the *Gnat1−/−* mouse model exhibits minimal changes in retinal ONL thickness up to 1 year of age, and no mRNA is produced from the knockout gene (12). Likewise, this cell death is unlikely to be a gene dosage effect since *Gnat1+/− rd10* mice undergo photoreceptor cell death at the same rate as *Gnat1−/− rd10* mice in light (unpublished data). The ONL thickness is also indistinguishable between *Gnat1+/− rd10* and littermate *rd10* mice when they are reared in the dark (unpublished data). Moreover, double and triple knockouts have been generated in previous studies without any noticeable effects on photoreceptor viability (26,27,56). Most notably, Fan *et al*. showed that the *Rpe65−/− Grk1−/− Gnat1−/−* triple knockout mouse model had increased photoreceptor survival in contrast to their *Rpe65−/− Grk1−/−* mouse model (26).

Future experiments will be needed to address the mechanisms underlying the neurodegeneration observed in the dark reared *Gnat1−/− rd10* mice. We suspect that some basal activity between transducin and PDE6 is required for photoreceptor survival to modulate the high intracellular Ca^{2+} levels observed in darkness (57). Interestingly, transducin is known to translocate to different subcellular locations of the photoreceptor cell depending on lighting conditions (58). In complete darkness, transducin is found in the OSs of rod photoreceptors, but upon exposure to light, it translocates and diffuses throughout the rod photoreceptor (58). Its sequestration to the OS only in darkness may allow for some basal activity that modulates high intracellular Ca^{2+} levels observed in darkness (57). Similarly, arrestin and Grb14 translocate from the IS in darkness to the OS upon light exposure, and this process is dependent on rhodopsin signaling yet independent of transducin signaling (59,60). Alternatively, in *Gnat1−/−* mice, intracellular Ca^{2+} concentrations do not undergo light-dependent reductions, and prolonged exposure to high Ca^{2+} levels may become toxic to photoreceptors (61). Another study also showed that oxidative stress is increased in *Gnat1−/−* mice, and this could be responsible for the underlying neurodegeneration observed (62). Future experiments

addressing the intracellular Ca^{2+} concentrations and oxidative stress in *Gnat1−/− rd10* mice will provide more insight into the mechanisms underlying the neurodegeneration observed.

In conclusion, this work shows for the first time that the signaling cascade responsible for the light-accelerated photoreceptor cell death in *rd10* mice relies on the rhodopsin GPCR but is independent of its G-protein transducin. However, future studies will be necessary to identify the transducin-independent signaling pathway, and whether or not rhodopsin is mediating light-induced photoreceptor cell death through an increased ion flux mechanism (15). It is tempting to speculate that if a protein downstream of rhodopsin can be identified and targeted for drug-mediated inhibition, patients with photoreceptor cell loss caused by light exposure can be treated while preserving their visual function.

Materials and Methods

Generation of mice and genotyping

Rd10 mice were obtained from the Jackson Laboratory in the *C57BL6/J* background. These mice were confirmed to be homozygous for the *rd10* allele and were bred with *Gnat1−/−* mice and *Rpe65−/−* mice that were kindly provided by Dr Vladimir Kefalov from Washington University with the approval of Dr Janis Lem from Tufts University. *Gnat1+/−rd10* and *Rpe65+/−rd10* strains were then separately crossed to generate *Rpe65−/−rd10* and *Gnat1−/−rd10* experimental mice, which were raised in rooms either in complete darkness or with a standard 12 h ∼175 lux light: 12 h dark cycle. Littermate *rd10* mice from these crosses were used as controls. The mouse models used for experimentation had no confounding *rd1* and *rd8* alleles (63,64). The genotype of offspring from breeding pairs was determined by polymerase chain reaction amplification of genomic DNA derived from ear biopsies. The *Rpe65* wild-type and null alleles were identified using the following primers (5′-TCA TGG TCT AGC CAT GTC TG-3′, 5′-CAC TTG TGT AGC GCC AAG TG-3′ and 5′-AAT CCC TAC CAG ATG CCA TC-3′) (65). The *Gnat1* wild-type and null alleles were identified by using the following primers (5′-TAT CCA CCA GGA CGG GTA TTC-3′, 5′-GCG GAG TCA TTG AGC TGG TAT-3′ and 5′-GGG AAC TTC CTG ACT AGG GGA GG-3′) (66). All experiments were conducted with the approval of the West Virginia University Institutional Animal Care and Use Committee, and all works were performed with adherence to the principles set forth in the ARVO Statement for the Ethical Use of Animals in Ophthalmic and Vision Research, which advocates minimum use of animals per study needed to obtain statistical significance.

Electroretinography

The ERG photoresponse was measured as previously described (67) using the UTAS BigShot LED Ganzfeld System with UBA-4204 amplifier and EM for Windows (LKC Technologies). After overnight dark adaptation, mice were placed under anesthesia using 1.5% isoflurane mixed with oxygen at 2 l/min. Electroretinograms (ERGs) from each eye were measured simultaneously from the corneal surface using electrodes after pupillary dilation with a 1:1 solution of 8% tropicamide: 1.5% phenylephrine hydrochloride. The electrodes were referenced to a needle electrode placed on the scalp between the ears. Hydroxypropyl methylcellulose (Novartis Pharmaceuticals) was added to facilitate contact between electrodes and the cornea while maintaining the integrity of the cornea. The mouse's body temperature was maintained at a temperature of 37°C using a regulated heating pad. Scotopic responses were obtained in complete darkness using single LED white light flashes of intensities varying from 2.45×10^{-4} to 2.4 cd-s/m^2. Photopic responses were obtained with single LED white light flashes after light adaptation using 30 cd-s/m^2 rod photoreceptor-saturating white light. The photoresponse versus flash intensity data was modeled using the Naka-Rushton fit as described previously (68).

Immunoblotting

Immunoblotting was performed using a protocol adapted from our laboratory (67). Briefly, mice were sacrificed using CO_2 followed by cervical dislocation, and retinas or whole eyes were frozen on dry ice for protein studies. Retinas or whole eyes were homogenized, and cells were lysed in phosphate buffered saline (PBS) supplemented with protease inhibitor and 0.1% 3-[(3-cholamidopropyl)dimethylammonio]-1-propanesulfonate (CHAPS) detergent by sonication. Cellular debris was cleared at 4°C by centrifugation for 10 min at 12 000*g*. The samples were placed into Laemmli buffer (2% SDS, 10% glycerol, 5% 2-mercaptoethanol, 0.002% bromophenol blue and 62.5 mM Tris–HCl pH 6.8) and boiled for 10 min before western blotting analysis. These lysates were loaded into standard SDS-PAGE gels and fractionated by size. The proteins were transferred onto PVDF membranes (Millipore) and subsequently blocked for 1 h with Odyssey Blocking Buffer (LICOR Biosciences) before incubation with primary antibody. The membranes were washed three times for 5 min in 0.1% Tween-20 in PBS, and secondary antibodies conjugated to infrared dye (Thermo-Fisher) were used to detect the primary antibody at 1:50 000 dilution. The membranes were then washed three times for 5 min in 0.1% Tween-20 in PBS and then scanned using an Odyssey Infrared Imaging System (LICOR Biosciences).

Immunofluorescence microscopy

Immunofluorescence microscopy was performed as previously described in our laboratory (67). Briefly, mice were sacrificed using CO_2 before secondary cervical dislocation. After enucleation of the eyes, the lens and cornea were removed. Eyes were immediately fixed by incubation in 4% paraformaldehyde in PBS for 1.5 h. Eyes were then incubated in 20% sucrose in PBS overnight after washing them three times in PBS for 5 min each. After placing the eyes in a 1:1 solution of optimal cutting temperature compound (OCT): 20% sucrose in PBS for 2 h, they were flash frozen in OCT (VWR). A Leica CM1850 cryostat was used to cryosection eyes at 16 µm thickness and collect retinal cross sections. The sections were placed on Superfrost Plus Slides (Fisher Scientific). Slides were then permeabilized with phosphate buffered saline supplemented with 0.1% Triton X-100 (PBST) and incubated for 30 min in a blocking buffer containing 0.05% sodium azide, 0.5% Triton X-100 and 10% goat serum in PBS. Retinal sections were incubated with primary antibody overnight at 4°C followed by three 5 min washes with PBST before incubation with secondary antibody and DAPI. After three 5 min washes in PBST and coverslip placement, a Nikon C2 Confocal Microscope was used to image slides.

Retinal histology of the *rd10* mice

Knockout and control mice were euthanized, and whole eyes were enucleated before marking the superior pole with a red

tissue dye (MarketLab), and eyes were then fixed for 48 h using Alcohol Z-fixative (Excalibur Pathology). Samples were then shipped to Excalibur Pathology for tissue processing and preparation of H&E stained slides. Images of stained slides were collected on a Nikon C2 Microscope using Elements software (Nikon). Images were processed using ImageJ software (National Institutes of Health).

PDE6 assembly assay by ROS1 pulldown

After euthanasia, retinas were isolated and frozen on dry ice before homogenization by sonication in co-immunoprecipitation buffer (20 mM Tris–HCl pH 8, 137 mM NaCl, 2 mM EDTA, 0.1% Triton X-100, 0.02% sodium azide, protease inhibitor cocktail and 10 mM iodoacetamide). Samples were centrifuged at 13 000*g* for 10 min at 4°C to remove debris. Lysates were then precleared by tumble incubation with protein A/G beads for 30 min at 4°C before centrifugation at 13 000*g* for 10 min. A total fraction was collected before tumble incubating samples with ROS1 monoclonal antibody for 4 h at 4°C. Samples were centrifuged at 13 000*g* for 10 min at 4°C. The supernatant was tumble incubated with protein A/G beads for 60 min at 4°C before centrifugation at 13 000*g* for 30 s. After collecting the unbound fraction, bead pellets were washed three times with washing buffer (10 mM Tris–HCl pH 7.4, 150 mM NaCl, 1 mM EDTA, 0.1% Triton X-100, 0.02% sodium azide and protease inhibitor cocktail). Laemmli buffer (2% SDS, 10% glycerol, 5% 2-mercaptoethanol, 0.002% bromophenol blue and 62.5 mM Tris–HCl pH 6.8) was then added to the beads, and samples were boiled for 5 min, lightly vortexed and subjected to centrifugation at 13 000*g* for 30 s. Samples from the total, unbound and bound fractions were then size fractionated on SDS-PAGE gels before immunoblotting as described earlier.

Antibodies

Throughout this work, the following primary antibodies were used at 1:1000 dilutions: rabbit anti-PDE6γ (Thermo-Fisher), rabbit anti-PDE6β (Thermo-Fisher), rabbit anti-PDE6α (Thermo-Fisher), anti-assembled PDE6 (i.e. ROS1) was a kind gift from Dr Ted Wensel from Baylor College and Rick Cote from University of New Hampshire, rabbit anti-rod-transducin-α (Santa Cruz), rabbit anti-RPE65 was a kind gift from Dr Michael Redmond from the National Eye Institute, mouse anti-glyceraldehyde 3-phosphate dehydrogenase (GAPDH; Fitzgerald), rhodamine peanut agglutinin (PNA: cone OS sheath marker, Vector Laboratories) and fluorescein WGA (rod OS sheath marker, Vector Laboratories).

Supplementary Material

Supplementary Material is available at *HMG* Online.

Acknowledgements

We thank Dr Michael Redmond for kindly providing us with an aliquot of anti-RPE65 antibody and Drs Vladimir Kefalov and Janis Lem for kindly providing us with the *Gnat1*−/− and *Rpe65*−/− knockout mice. We also thank Drs Ted Wensel and Rick Cote for providing us with the ROS1 antibody.

Funding

The National Institutes of Health (grant numbers RO1 EY028035, R01 EY025536 and R21 EY027707); the West Virginia Lions Club Foundation; International Lions Club Foundation.

Conflict of Interest Statement

The authors have no conflicts of interest.

References

1. Fahim, A.T., Daiger, S.P. and Weleber, R.G. (2017) Nonsyndromic retinitis pigmentosa overview. In Adam MP, HH Ardinger, Pagon RA and Wallace SE ed. *GeneReviews® [Internet]*. University of Washington, Seattle. pp. 1–46.
2. Ferrari, S., Di Iorio, E., Barbaro, V., Ponzin, D., Sorrentino, F.S. and Parmeggiani, F. (2011) Retinitis pigmentosa: genes and disease mechanisms. *Curr. Genomics*, **12**, 238–249.
3. Hartong, D.T., Berson, E.L. and Dryja, T.P. (2006) Retinitis pigmentosa. *Lancet*, **368**, 1795–1809.
4. Geruschat, D. and Turano, K. (2002) Connecting research on retinitis pigmentosa to the practice of orientation and mobility. *J. Vis. Impair. Blind.*, **96**, 69–85.
5. Chang, B., Hawes, N.L., Pardue, M.T., German, A.M., Hurd, R.E., Davisson, M.T., Nusinowitz, S., Rengarajan, K., Boyd, A.P., Sidney, S.S. *et al.* (2007) Two mouse retinal degenerations caused by missense mutations in the β-subunit of rod cGMP phosphodiesterase gene. *Vis. Res.*, **47**, 624–633.
6. Kiser, P.D. and Palczewski, K. (2010) Membrane-binding and enzymatic properties of RPE65. *Prog. Retin. Eye Res.*, **29**, 428–442.
7. Huang, J., Possin, D.E. and Saari, J.C. (2009) Localizations of visual cycle components in retinal pigment epithelium. *Mol. Vis.*, **15**, 223–234.
8. Parker, R.O. and Crouch, R.K. (2010) Retinol dehydrogenases (RDHs) in the visual cycle. *Exp. Eye Res.*, **91**, 788–792.
9. Moiseyev, G., Chen, Y., Takahashi, Y., Wu, B.X. and Ma, J.X. (2005) RPE65 is the isomerohydrolase in the retinoid visual cycle. *Proc. Natl. Acad. Sci. USA*, **102**, 12413–12418.
10. Redmond, T.M., Yu, S., Lee, E., Bok, D., Hamasaki, D., Chen, N., Goletz, P., Ma, J.X., Crouch, R.K. and Pfeifer, K. (1998) Rpe65 is necessary for production of 11-cis-vitamin A in the retinal visual cycle. *Nat. Genet.*, **20**, 344–351.
11. Grimm, C., Wenzel, A., Hafezi, F., Yu, S., Redmond, T.M. and Remé, C.E. (2000) Protection of Rpe65-deficient mice identifies rhodopsin as a mediator of light-induced retinal degeneration. *Nat. Genet.*, **25**, 63–66.
12. Calvert, P.D., Krasnoperova, N.V., Lyubarsky, A.L., Isayama, T., Nicolo, M., Kosaras, B., Wong, G., Gannon, K.S., Margolskee, R.F., Sidman, R.L. *et al.* (2000) Phototransduction in transgenic mice after targeted deletion of the rod transducin α-subunit. *Proc. Natl. Acad. Sci. USA*, **97**, 13913–13918.
13. Humphries, M.M., Rancourt, D., Farrar, G.J., Kenna, P., Hazel, M., Bush, R.A., Sieving, P.A., Sheils, D.M., Creighton, P., Erven, A. *et al.* (1997) Retinopathy induced in mice by targeted disruption of the rhodopsin gene. *Nat. Genet.*, **15**, 216–219.
14. Kolandaivelu, S., Huang, J., Hurley, J.B. and Ramamurthy, V. (2009) AIPL1, a protein associated with childhood blindness, interacts with α-subunit of rod phosphodiesterase (PDE6) and is essential for its proper assembly. *J. Biol. Chem.*, **284**, 30853–30861.
15. Wang, T., Reingruber, J., Woodruff, M.L., Majumder, A., Camarena, A., Artemyev, N.O., Fain, G.L. and Chen, J. (2018)

The PDE6 mutation in the rd10 retinal degeneration mouse model causes protein mislocalization and instability and promotes cell death through increased ion influx. *J. Biol. Chem.*, **293**, 15332–15346.
16. Paquet-Durand, F., Beck, S., Michalakis, S., Goldmann, T., Huber, G., Mühlfriedel, R., Trifunović, D., Fischer, M.D., Fahl, E., Duetsch, G. *et al.* (2010) A key role for cyclic nucleotide gated (CNG) channels in cGMP-related retinitis pigmentosa. *Hum. Mol. Genet.*, **20**, 941–947.
17. Tsang, S.H., Gouras, P., Yamashita, C.K., Kjeldbye, H., Fisher, J., Farber, D.B. and Goff, S.P. (1996) Retinal degeneration in mice lacking the γ subunit of the rod cGMP phosphodiesterase. *Science*, **272**, 1026–1029.
18. Dvir, L., Srour, G., Abu-Ras, R., Miller, B., Shalev, S.A. and Ben-Yosef, T. (2010) Autosomal-recessive early-onset retinitis pigmentosa caused by a mutation in PDE6G, the gene encoding the gamma subunit of rod cGMP phosphodiesterase. *Am. J. Hum. Genet.*, **87**, 258–264.
19. Lobanova, E.S., Finkelstein, S., Skiba, N.P. and Arshavsky, V.Y. (2013) Proteasome overload is a common stress factor in multiple forms of inherited retinal degeneration. *Proc. Natl. Acad. Sci. USA*, **110**, 9986–9991.
20. Weiss, E.R., Heller-Harrison, R.A., Diez, E., Crasnier, M., Malbon, C.C. and Johnson, G.L. (1990) Rhodopsin expressed in Chinese hamster ovary cells regulates adenylyl cyclase activity. *J. Mol. Endocrinol.*, **4**, 71–79.
21. Weiss, E.R., Hao, Y., Dickerson, C.D., Osawa, S., Shi, W., Zhang, L.R. and Wong, F. (1995) Altered cAMP levels in retinas from transgenic mice expressing a rhodopsin mutant. *Biochem. Biophys. Res. Commun.*, **216**, 755–761.
22. Li, X., Gutierrez, D.V., Hanson, M.G., Han, J., Mark, M.D., Chiel, H., Hegemann, P., Landmesser, L.T. and Herlitze, S. (2005) Fast noninvasive activation and inhibition of neural and network activity by vertebrate rhodopsin and green algae channelrhodopsin. *Proc. Natl. Acad. Sci. USA*, **102**, 17816–17821.
23. Kanaho, Y., Tsai, S.C., Adamik, R., Hewlett, E.L., Moss, J. and Vaughan, M. (1984) Rhodopsin-enhanced GTPase activity of the inhibitory GTP-binding protein of adenylate cyclase. *J. Biol. Chem.*, **259**, 7378–7381.
24. Alfinito, P.D. and Townes-Anderson, E. (2002) Activation of mislocalized opsin kills rod cells: a novel mechanism for rod cell death in retinal disease. *Proc. Natl. Acad. Sci. USA*, **99**, 5655–5660.
25. Campbell, A.P. and Smrcka, A.V. (2018) Targeting G protein-coupled receptor signalling by blocking G proteins. *Nat. Rev. Drug Discov.*, **17**, 789–803.
26. Fan, J., Sakurai, K., Chen, C.K., Rohrer, B., Wu, B.X., Yau, K.W., Kefalov, V. and Crouch, R.K. (2010) Deletion of GRK1 causes retina degeneration through a transducin-independent mechanism. *J. Neurosci.*, **30**, 2496–2503.
27. Hao, W., Wenzel, A., Obin, M.S., Chen, C.K., Brill, E., Krasnoperova, N.V., Eversole-Cire, P., Kleyner, Y., Taylor, A., Simon, M.I. *et al.* (2002) Evidence for two apoptotic pathways in light-induced retinal degeneration. *Nat. Genet.*, **32**, 254–260.
28. Brockerhoff, S.E., Rieke, F., Matthews, H.R., Taylor, M.R., Kennedy, B., Ankoudinova, I., Niemi, G.A., Tucker, C.L., Xiao, M., Cilluffo, M.C. *et al.* (2003) Light stimulates a transducin-independent increase of cytoplasmic Ca2+ and suppression of current in cones from the zebrafish mutant nof. *J. Neurosci.*, **23**, 470–480.
29. Osawa, S., Jo, R., Xiong, Y., Reidel, B., Tserentsoodol, N., Arshavsky, V.Y., Iuvone, P.M. and Weiss, E.R. (2011) Phosphorylation of G protein-coupled receptor kinase 1 (GRK1) is regulated by light but independent of phototransduction in rod photoreceptors. *J. Biol. Chem.*, **286**, 20923–20929.
30. Rajala, A., Anderson, R.E., Ma, J.X., Lem, J., Al-Ubaidi, M.R. and Rajala, R.V. (2007) G-protein-coupled receptor rhodopsin regulates the phosphorylation of retinal insulin receptor. *J. Biol. Chem.*, **282**, 9865–9873.
31. Rajala, A., Tanito, M., Le, Y.Z., Kahn, C.R. and Rajala, R.V. (2008) Loss of neuroprotective survival signal in mice lacking insulin receptor gene in rod photoreceptor cells. *J. Biol. Chem.*, **283**, 19781–19792.
32. Gupta, V.K., Rajala, A. and Rajala, R.V. (2012) Insulin receptor regulates photoreceptor CNG channel activity. *Am. J. Physiol. Endocrinol. Metab.*, **303**, E1363–E1372.
33. Guo, C., Otani, A., Oishi, A., Kojima, H., Makiyama, Y., Nakagawa, S. and Yoshimura, N. (2012) Knockout of ccr2 alleviates photoreceptor cell death in a model of retinitis pigmentosa. *Exp. Eye Res.*, **104**, 39–47.
34. Strettoi, E., Gargini, C., Novelli, E., Sala, G., Piano, I., Gasco, P. and Ghidoni, R. (2010) Inhibition of ceramide biosynthesis preserves photoreceptor structure and function in a mouse model of retinitis pigmentosa. *Proc. Natl. Acad. Sci. USA*, **107**, 18706–18711.
35. Xu, L., Kong, L., Wang, J. and Ash, J.D. (2018) Stimulation of AMPK prevents degeneration of photoreceptors and the retinal pigment epithelium. *Proc. Natl. Acad. Sci. USA*, **115**, 10475–10480.
36. Patel, A.K., Surapaneni, K., Yi, H., Nakamura, R.E., Karli, S.Z., Syeda, S., Lee, T. and Hackam, A.S. (2015) Activation of Wnt/β-catenin signaling in Muller glia protects photoreceptors in a mouse model of inherited retinal degeneration. *Neuropharmacology*, **91**, 1–12.
37. Platón-Corchado, M., Barcelona, P.F., Jmaeff, S., Marchena, M., Hernández-Pinto, A.M., Hernández-Sánchez, C., Saragovi, H.U. and De La Rosa, E.J. (2017) p75 NTR antagonists attenuate photoreceptor cell loss in murine models of retinitis pigmentosa. *Cell Death Dis.*, **8**, e2922.
38. de la Cámara, C.M.F., Hernández-Pinto, A.M., Olivares-González, L., Cuevas-Martín, C., Sánchez-Aragó, M., Hervás, D., Salom, D., Cuezva, J.M., Enrique, J., Millán, J.M. *et al.* (2015) Adalimumab reduces photoreceptor cell death in a mouse model of retinal degeneration. *Sci. Rep.*, **5**, 11764–11777.
39. Xiang, Z., Bao, Y., Zhang, J., Liu, C., Xu, D., Liu, F., Chen, H., He, L., Ramakrishna, S., Zhang, Z. *et al.* (2018) Inhibition of non-NMDA ionotropic glutamate receptors delays the retinal degeneration in rd10 mouse. *Neuropharmacology*, **139**, 137–149.
40. Rodriguez-Muela, N., Hernandez-Pinto, A.M., Serrano-Puebla, A., Garcia-Ledo, L., Latorre, S.H., De La, E.J. and Boya, P. (2015) Lysosomal membrane permeabilization and autophagy blockade contribute to photoreceptor cell death in a mouse model of retinitis pigmentosa. *Cell Death Differ.*, **22**, 476–487.
41. Nakao, T., Tsujikawa, M., Notomi, S., Ikeda, Y. and Nishida, K. (2012) The role of mislocalized phototransduction in photoreceptor cell death of retinitis pigmentosa. *PLoS One*, **7**, e32472.
42. Isiegas, C., Marinich-Madzarevich, J.A., Marchena, M., Ruiz, J.M., Cano, M.J., de la Villa, P., Hernández-Sánchez, C., Enrique, J. and de Pablo, F. (2016) Intravitreal injection of proinsulin-loaded microspheres delays photoreceptor cell death and vision loss in the rd10 mouse model of retinitis pigmentosa. *Invest. Ophthalmol. Vis. Sci.*, **57**, 3610–3618.

43. Arroba, A.I., Álvarez-Lindo, N., Van Rooijen, N. and Enrique, J. (2011) Microglia-mediated IGF-I neuroprotection in the rd10 mouse model of retinitis pigmentosa. *Invest. Ophthalmol. Vis. Sci.*, **52**, 9124–9130.
44. Zhao, L., Zabel, M.K., Wang, X., Ma, W., Shah, P., Fariss, R.N., Qian, H., Parkhurst, C.N., Gan, W.B. and Wong, W.T. (2015) Microglial phagocytosis of living photoreceptors contributes to inherited retinal degeneration. *EMBO Mol. Med.*, **7**, 1179–1197.
45. Sasahara, M., Otani, A., Oishi, A., Kojima, H., Yodoi, Y., Kameda, T., Nakamura, H. and Yoshimura, N. (2008) Activation of bone marrow-derived microglia promotes photoreceptor survival in inherited retinal degeneration. *Am. J. Pathol.*, **172**, 1693–1703.
46. Wang, X., Zhao, L., Zhang, Y., Ma, W., Gonzalez, S.R., Fan, J., Kretschmer, F., Badea, T.C., Qian, H.H. and Wong, W.T. (2017) Tamoxifen provides structural and functional rescue in murine models of photoreceptor degeneration. *J. Neurosci.*, **37**, 3294–3310.
47. Phillips, M.J., Walker, T.A., Choi, H.Y., Faulkner, A.E., Kim, M.K., Sidney, S.S., Boyd, A.P., Nickerson, J.M., Boatright, J.H. and Pardue, M.T. (2008) Tauroursodeoxycholic acid preservation of photoreceptor structure and function in the rd10 mouse through postnatal day 30. *Invest. Ophthalmol. Vis. Sci.*, **49**, 2148–2155.
48. Kang, K., Tarchick, M.J., Yu, X., Beight, C., Bu, P. and Yu, M. (2016) Carnosic acid slows photoreceptor degeneration in the Pde6b rd10 mouse model of retinitis pigmentosa. *Sci. Rep.*, **6**, 22632–22643.
49. Doonan, F., O'Driscoll, C., Kenna, P. and Cotter, T.G. (2011) Enhancing survival of photoreceptor cells in vivo using the synthetic progestin Norgestrel. *J. Neurochem.*, **118**, 915–927.
50. Komeima, K., Rogers, B.S. and Campochiaro, P.A. (2007) Antioxidants slow photoreceptor cell death in mouse models of retinitis pigmentosa. *J. Cell. Physiol.*, **213**, 809–815.
51. Picard, E., Jonet, L., Sergeant, C., Vesvres, M.H., Behar-Cohen, F., Courtois, Y. and Jeanny, J.C. (2010) Overexpressed or intraperitoneally injected human transferrin prevents photoreceptor degeneration in rd10 mice. *Mol. Vis.*, **16**, 2612–2625.
52. Obolensky, A., Berenshtein, E., Lederman, M., Bulvik, B., Alper-Pinus, R., Yaul, R., Deleon, E., Chowers, I., Chevion, M. and Banin, E. (2011) Zinc–desferrioxamine attenuates retinal degeneration in the rd10 mouse model of retinitis pigmentosa. *Free Radic. Biol. Med.*, **51**, 1482–1491.
53. Ikeda, H.O., Sasaoka, N., Koike, M., Nakano, N., Muraoka, Y., Toda, Y., Fuchigami, T., Shudo, T., Iwata, A., Hori, S. *et al.* (2014) Novel VCP modulators mitigate major pathologies of rd10, a mouse model of retinitis pigmentosa. *Sci. Rep.*, **4**, 5970–5979.
54. Barone, I., Novelli, E., Piano, I., Gargini, C. and Strettoi, E. (2012) Environmental enrichment extends photoreceptor survival and visual function in a mouse model of retinitis pigmentosa. *PLoS One*, **7**, e50726.
55. Barone, I., Novelli, E. and Strettoi, E. (2014) Long-term preservation of cone photoreceptors and visual acuity in rd10 mutant mice exposed to continuous environmental enrichment. *Mol. Vis.*, **20**, 1545–1556.
56. Hattar, S., Lucas, R.J., Mrosovsky, N., Thompson, S., Douglas, R.H., Hankins, M.W., Lem, J., Biel, M., Hofmann, F., Foster, R.G. *et al.* (2003) Melanopsin and rod–cone photoreceptive systems account for all major accessory visual functions in mice. *Nature*, **424**, 75–81.
57. Krizaj, D. and Copenhagen, D.R. (2002) Calcium regulation in photoreceptors. *Front. Biosci. J. Virtual Lib.*, **7**, d2023–d2044.
58. Sokolov, M., Lyubarsky, A.L., Strissel, K.J., Savchenko, A.B., Govardovskii, V.I., Pugh, E.N., Jr. and Arshavsky, V.Y. (2002) Massive light-driven translocation of transducin between the two major compartments of rod cells: a novel mechanism of light adaptation. *Neuron*, **34**, 95–106.
59. Mendez, A., Lem, J., Simon, M. and Chen, J. (2003) Light-dependent translocation of arrestin in the absence of rhodopsin phosphorylation and transducin signaling. *J. Neurosci.*, **23**, 3124–3129.
60. Rajala, A., Daly, R.J., Tanito, M., Allen, D.T., Holt, L.J., Lobanova, E.S., Arshavsky, V.Y. and Rajala, R.V. (2009) Growth factor receptor-bound protein 14 undergoes light-dependent intracellular translocation in rod photoreceptors: functional role in retinal insulin receptor activation. *Biochemistry*, **48**, 5563–5572.
61. Woodruff, M.L., Sampath, A.P., Matthews, H.R., Krasnoperova, N.V., Lem, J. and Fain, G.L. (2002) Measurement of cytoplasmic calcium concentration in the rods of wild-type and transducin knock-out mice. *J. Physiol.*, **542**, 843–854.
62. Berkowitz, B.A., Lewin, A.S., Biswal, M.R., Bredell, B.X., Davis, C. and Roberts, R. (2016) MRI of retinal free radical production with laminar resolution in vivo. *Invest. Ophthalmol. Vis. Sci.*, **57**, 577–585.
63. Gimenez, E. and Montoliu, L. (2001) A simple polymerase chain reaction assay for genotyping the retinal degeneration mutation (Pdebrd1) in FVB/N-derived transgenic mice. *Lab. Anim.*, **35**, 153–156.
64. Pak, J.S., Lee, E.J. and Craft, C.M. (2015) The retinal phenotype of Grk1−/− is compromised by a Crb1rd8 mutation. *Mol. Vis.*, **21**, 1281–1294.
65. Cottet, S., Jüttner, R., Voirol, N., Chambon, P., Rathjen, F.G., Schorderet, D.F. and Escher, P. (2013) Retinal pigment epithelium protein of 65 kDA gene-linked retinal degeneration is not modulated by chicken acidic leucine-rich epidermal growth factor-like domain containing brain protein/Neuroglycan C/chondroitin sulfate proteoglycan 5. *Mol. Vis.*, **19**, 2312–2320.
66. Tracy, C.M., Kolesnikov, A.V., Blake, D.R., Chen, C.K., Baehr, W., Kefalov, V.J. and Willardson, B.M. (2015) Retinal cone photoreceptors require phosducin-like protein 1 for G protein complex assembly and signaling. *PloS One*, **10**, e0117129.
67. Wright, Z.C., Singh, R.K., Alpino, R., Goldberg, A.F., Sokolov, M. and Ramamurthy, V. (2016) ARL3 regulates trafficking of prenylated phototransduction proteins to the rod outer segment. *Hum. Mol. Genet.*, **25**, 2031–2044.
68. Severns, M.L. and Johnson, M.A. (1993) The care and fitting of Naka-Rushton functions to electroretinographic intensity-response data. *Doc. Ophthalmol.*, **85**, 135–150.